



**Universiteit
Leiden**
The Netherlands

Artificial intelligence modelling of tyrosine kinase inhibitors at risk of malabsorption and bioavailability-enhancing strategies

Huntjens, D.W.; Béquignon, O.J.M.; Krens, S.D.; Löwenberg, M.; Chamuleau, M.E.D.; Molenaar, R.J.; ... ; Bartelink, I.H.

Citation

Huntjens, D. W., Béquignon, O. J. M., Krens, S. D., Löwenberg, M., Chamuleau, M. E. D., Molenaar, R. J., ... Bartelink, I. H. (2025). Artificial intelligence modelling of tyrosine kinase inhibitors at risk of malabsorption and bioavailability-enhancing strategies. *British Journal Of Clinical Pharmacology*, 91(11), 3130-3140. doi:10.1002/bcp.70166

Version: Publisher's Version




License: [Creative Commons CC BY-NC 4.0 license](https://creativecommons.org/licenses/by-nc/4.0/)

Downloaded from: <https://hdl.handle.net/1887/4285224>

Note: To cite this publication please use the final published version (if applicable).

ORIGINAL ARTICLE

Artificial intelligence modelling of tyrosine kinase inhibitors at risk of malabsorption and bioavailability-enhancing strategies

Daan W. Huntjens¹  | Olivier J. M. Béquignon^{2,3}  | Stefanie D. Krens¹  |
 Mark Löwenberg⁴  | Martine E. D. Chamuleau^{3,5}  | Remco J. Molenaar⁵  |
 Anita M. G. Kramers⁵ | Marianne A. Kuijvenhoven¹  | Imke H. Bartelink^{1,3} 

¹Pharmacy & Clinical Pharmacology, Amsterdam University Medical Center, Amsterdam, The Netherlands

²Department of Neurosurgery, Amsterdam University Medical Center, Amsterdam, The Netherlands

³Cancer Center Amsterdam, Cancer treatment and Quality of Life, Amsterdam, The Netherlands

⁴Department of Gastroenterology and Hepatology, Amsterdam University Medical Center, The Netherlands

⁵Department of Hematology, Amsterdam University Medical Center, The Netherlands

Correspondence

Daan W. Huntjens, Pharmacy & Clinical Pharmacology, Amsterdam University Medical Center, Amsterdam, The Netherlands.
 Email: d.huntjens@amsterdamumc.nl

Funding information

This research received no specific grant from any funding agency in the public, commercial, or not-for-profit sectors.

Aims: The study aims to predict and improve the absorption of tyrosine kinase inhibitors (TKIs) in patients with malabsorption issues, particularly those who have undergone bariatric surgery or are using proton-pump inhibitors. The research involves 2 main components: the development of an artificial intelligence (AI) model to identify TKIs that are susceptible to reduced absorption in these patients, and the application of case-specific absorption enhancements based on 2 clinical scenarios.

Methods: A fully connected neural network was applied using pH-dependent solubility data from 137 785 compounds to identify TKIs at risk of reduced bioavailability when bypassing the stomach. The clinical impact of gastric acid suppressants on the bioavailability of 71 approved TKIs was evaluated by correlating the AI solubility estimates with the effect of proton-pump inhibitors on clinical exposure. Furthermore, absorption enhancement was applied in 2 clinical scenarios, with therapeutic drug monitoring assessing the effectiveness of the enhancement.

Results: Two AI models were developed to predict the difference in molecular aqueous solubility between acid and neutral pH and to capture the concentration available for intestinal absorption in healthy and in patients with malabsorption issues. The AI model capturing the solubility difference between acidic and neutral pH demonstrated predictive capabilities, with a Pearson correlation coefficient of .95 and a coefficient of determination of .90. It predicted that the solubility difference, between acidic and neutral pH, was associated with clinical bioavailability ($P < .001$). Nilotinib, lapatinib and dacomitinib were ranked as TKIs with the highest risk of malabsorption in case of increased stomach pH.

Conclusion: We developed an AI-based model that predicts TKIs that are at risk of malabsorption when bypassing the stomach or used with gastric acid suppressants. Drugs with a high malabsorption risk can be enhanced by various methods to improve bioavailability.

The authors confirm that the Principal Investigator for this paper is Imke Bartelink and that she had direct clinical responsibility for patients.

Daan W. Huntjens and Olivier J. M. Béquignon, these authors contributed equally to this work.

This is an open access article under the terms of the [Creative Commons Attribution-NonCommercial](https://creativecommons.org/licenses/by-nc/4.0/) License, which permits use, distribution and reproduction in any medium, provided the original work is properly cited and is not used for commercial purposes.

© 2025 The Author(s). *British Journal of Clinical Pharmacology* published by John Wiley & Sons Ltd on behalf of British Pharmacological Society.

KEYWORDS

absorption enhancement, artificial intelligence, bioavailability, pharmacokinetics, pH-dependent solubility, therapeutic drug monitoring, tyrosine kinase inhibitors

1 | INTRODUCTION

Tyrosine kinase inhibitors (TKIs) are a class of drugs that target specific enzymes that play essential roles in signalling and are involved in various cellular processes. TKIs are potent therapies for various diseases, including solid tumours, haematological malignancies and immune-mediated inflammatory diseases such as rheumatic arthritis and inflammatory bowel disease. These drugs are typically administered orally, thereby allowing long-term treatment, increasing accessibility and patient comfort. Although TKIs have revolutionized the treatment of diseases such as chronic myeloid leukaemia and BCR::ABL1-positive B-cell acute lymphoblastic leukaemia (B-ALL), treatment with TKIs is sometimes challenging because of their limited bioavailability due to poor solubility.¹ Most TKIs are available only as oral formulations. The lack of other administration routes may limit their use in patients who cannot swallow, for example, because of mucositis or vomiting, and in specific clinical conditions such as postgastric (bypass) surgery or intubated patients.²

Drug absorption is the process by which a drug enters the systemic circulation from the site of administration. Several factors influence drug absorption, including physicochemical properties, pharmaceutical formulation, enterohepatic circulation, coadministration with other drugs and physiological factors. Physicochemical properties, such as solubility, molecular weight, lipophilicity and charge of the molecule, affect drug absorption. Before oral absorption, the drug must dissolve in the fluids of the gastrointestinal tract.³ Lipophilic and nonionized molecules tend to dissolve slowly in these fluids but are absorbed more readily than hydrophilic and ionized molecules. Generally, TKIs exhibit weak basicity and hydrophobicity. Therefore, most TKIs are not readily soluble in the gastrointestinal tract, except in the highly acidic environment of the stomach where the TKIs are in their ionized form.⁴ Drug–drug interactions (DDIs) with proton-pump inhibitors (PPIs) and antacids or food intake may affect bioavailability.⁵ Pharmaceutical formulations include a specific composition and design of the drug product. These include the dosage forms, excipients and coatings. Finally, physiological factors can affect drug absorption. For example, increased or decreased blood flow, limited surface area for absorption after gastric surgery, food intake, pH of the enteral environment, gastroenteric tube placement and the presence and capacity of transporters or enzymes (including other drugs that induce or inhibit these transporters or enzymes) in the membranes can affect drug absorption.

The Biopharmaceutics Classification System (BCS) categorizes drugs based on their solubility and permeability using *in vitro* measurements of permeability and solubility.⁶ Solubility refers to the ability of a drug to dissolve in gastrointestinal (GI) fluids, whereas permeability refers to its ability to cross biological membranes. TKIs are mostly categorized as BCS class II or IV and are characterized by

What is already known about this subject

- In clinical practice, the bioavailability of tyrosine kinase inhibitors (TKIs) can be challenging in patients with altered gastrointestinal absorption (e.g. swallowing disorders, feeding tubes, or gastric bypass surgery) or are receiving gastric acid suppression therapy with proton-pump inhibitors.
- Weak basic TKIs have limited solubility in the gastrointestinal tract, except in the highly acidic environment of the stomach, where they remain in their ionized form, resulting in increased solubility.
- The identification of drugs influenced by altered absorption processes is crucial because low exposure to most TKIs has been associated with lower overall survival.

What this study adds

- We developed an artificial intelligence model to identify TKIs at risk of malabsorption when bypassing the stomach or when coadministered with gastric acid suppressants.
- The artificial intelligence model performed well in correlating the predicted difference in solubility between acidic and neutral pH and the clinical bioavailability when exposed to gastric acid suppressants
- We share several strategies to enhance bioavailability for TKIs that are subject to malabsorption (e.g. dissolving TKIs in tube feeding or cola) using a multidisciplinary approach with insights from pharmacists, chemists, haematologists and gastroenterologists.

low solubility. The absorption of TKIs is probably affected by differences in their solubility in the GI tract. These drugs can be affected by changes in the physiology of GI fluids such as pH, buffer capacity and ionic strength. We hypothesize that, as BCS is determined only in healthy patients, TKIs' bioavailability could be compromised in patients with GI pH disturbances, for example, due to gastric (bypass) surgery. Two examples are dasatinib and ibrutinib, both BCS class II TKIs, with limited dissolution rates due to their low solubility at neutral pH, potentially affecting their absorption.

Machine-based learning methods have been applied to predict the aqueous solubility of small uncharged molecules with a relatively

good prediction performance,⁷ and so-called deep learning has become increasingly popular.^{8–11} Solubility is easier to assess than bioavailability. Therefore, most methodologies focus on either predicting the intrinsic solubility of molecules, the measured solubility at the solvation equilibrium between the dissolved and the solid state at a pH where the compound is fully neutral, or on the solubility at physiological pH between 7.0 and 7.4. The prediction of pH-dependent solubility using machine learning has long been overlooked, and only recently have models been derived using undisclosed data.¹²

Identification of drugs that are influenced by altered absorption processes is crucial because low exposure to most TKIs is associated with decreased efficacy in patients suffering from various cancers.¹³ Therefore, this study aims to predict and improve the absorption of TKIs in patients with malabsorption issues, particularly those who have undergone bariatric surgery or are using proton-pump inhibitors (PPIs) as reduced pH or gastric function may reduce TKI absorption. The research involves 2 main components: the development of an artificial intelligence (AI) model to identify TKIs that are susceptible to reduced absorption in these patients, and the application of case-specific absorption enhancements based on 2 clinical scenarios. These findings may provide healthcare practitioners with valuable insights into the clinical decision-making processes.

2 | METHODS

2.1 | Developing an AI model to identify TKIs that are susceptible to reduced absorption in patients who have undergone bariatric surgery or are using PPIs

An AI solution to identify TKIs at risk of reduced bioavailability when bypassing the stomach was developed by combining the clinical and intrinsic chemical data of 71 licensed TKIs. This AI solution is based on 2 models: the first predicts solubility at neutral pH, which represents the pH along most of the GI tract, and the second predicts the difference in solubility between neutral and acidic pH, characterizing the effect of pH on TKI absorption.

To develop the first model, denoted as FCNN_{neutral}, experimental aqueous solubility data, expressed as the negative decadic logarithm of molar concentrations, were obtained from the Online Chemical Modelling Environment¹⁴ for a total of 164 290 compounds. Only values obtained at neutral pH (pH = 7.4) were kept, duplicates were removed and compounds with multiple experimental solubilities were filtered out.

In total, 110 023 compounds were excluded from the filtering. Mold2,¹⁵ PaDEL,¹⁶ ChemoPy,¹⁷ the Chemistry Development Kit (CDK)¹⁸ and BlueDesc molecular descriptors were obtained for the remaining 54 267 nonstandardized molecules to encompass as many salt forms and formulations as possible. Aberrant values, with absolute values >100 000, were set to 0. To avoid data leakage during the training of the model, the dataset was randomly split into training, validation and holdout test sets, using a 7:1:2 ratio, based on the compounds' unique InChIKeys after standardization using the Papyrus

structure pipeline (version 0.0.5).¹⁹ To further assess the capability of the model to predict new chemical series, the data were split into training, validation and holdout test sets using the RDKit implementation of Bemis–Murcko scaffolds with similar ratios as for the random split. Training sets were normalized using standard scaling, and features with a standard deviation <0.10 were removed. The validation and holdout test sets were preprocessed according to their corresponding training sets.

To develop the second model, denoted as FCNN_{ΔlogS}, aqueous pH-dependent solubility, expressed as the non-negative decadic logarithm of molar concentrations, was obtained from the ChemAxon solubility predictor plugin for 137 793 compounds of the Asinex vendor catalogue. Molecules with constant pH solubilities throughout the pH range were discarded. Differences in solubility between neutral (pH = 7.4) and acidic (pH = 1.0) pH (ΔlogS) were derived for the remaining 137 785 molecules and were used as the dependent variable to be predicted. For the first model, Mold2, PaDEL, ChemoPy, CDK and BlueDesc molecular descriptors were obtained for the molecules, but after standardization with the Papyrus structure pipeline. Training, validation and holdout test sets were derived using both a random and a scaffold splitting scheme, as previously mentioned, using similar ratios. For both the random and scaffold splits, each feature of the training sets was scaled by its maximum absolute value, and features with a standard deviation <0.10 were removed. The validation and holdout test sets were preprocessed according to their corresponding training sets.

Both models consisted of fully connected neural networks (FCNNs) as their performance was much higher than other types of models—e.g. random forest or gradient-boosted decision trees—in our preliminary testing. These FCNN models were fitted to the data of the training sets. To determine the best set of hyperparameters for these models, a parameter sweep minimizing the models' prediction error on the validation sets after 100 epochs, each representing 1 complete iteration through all training data, was carried out. This ensured that the model size was minimal but predictive and would extrapolate well to new data. As a result of the hyperparameter optimization, both models consisted of 3 hidden layers with 1000, 200 and 100 neurons respectively, with the rectified linear unit (ReLU) being used as an activation function activation, dropout rates of 10% for FCNN_{neutral} and 5% for FCNN_{ΔlogS}, and the Adam optimizer with a learning rate of 0.0001 being chosen. The FCNN models were fitted until convergence which was determined by the maximization of the Pearson correlation coefficient on the validation sets. To avoid training for an extended time with negligible improvement in performance, early stopping was used with a patience of 500 epochs and a warm-up stage of 1000 training epochs. The warming-up stage ensured the models reached satisfactory performance and patience, that given no improvement for 500 epochs, the training would stop.

External validation of the machine learning model was performed by comparing the predicted solubility—both at neutral and acid pH—and the predicted difference in solubility (ΔlogS) with 4 clinically relevant variables as reported by the Food and Drugs Administration

(FDA)/European Medicines Agency (EMA)/Therapeutic Goods Administration (TGA; Appendix; and in case of missing data, literature reports were added): BSC classification (4 classes and I/III vs II/IV), in vitro derived pH-dependent solubility (yes/no), strong/weak base (strong bases are compounds that gain hydrogens with a $pK_a > 7$;²⁰ Clinical validation was performed by comparing the model's results with clinical trial data on the effect of PPI coadministration on drug exposure, as reported in the FDA, EMA and TGA assessments of 71 marketed tyrosine kinase inhibitors or published clinical trials. These data were obtained from distinct cohorts, each consisting of numerous patients. The difference in the area under the concentration–time profile (AUC) was used as a measure of bioavailability to assess the acid-suppressive effect. The results were classified as low when the AUC decrease was $<25\%$, medium if the AUC decrease was $25\text{--}50\%$ and high if the AUC decrease was $>50\%$. As a positive control, model predictions of acidic compounds (non-TKIs), for which acid-suppressive agents may have a positive antiacid effect on exposure, were included. We considered the model adequate if we could identify the molecular structure related to pH-dependent absorption in 80% of TKI and could pinpoint the main reasons for failure in the other (max 20%).

2.2 | Application of case-specific absorption enhancements based on 2 clinical cases (Box)

To demonstrate our clinical experience, we describe 2 patients who exhibited challenges in the absorption of TKIs and a method to assess their bioavailability using therapeutic drug monitoring (TDM).

2.3 | Case presentation

Box Case 1: Ibrutinib

A 60-year-old male with Waldenström macroglobulinaemia, a type of non-Hodgkin lymphoma, and poor response after 5 cycles of dexamethasone, rituximab and cyclophosphamide therapy, was switched to ibrutinib. His medical history included tonsillar carcinoma treated with chemoradiotherapy, complicated by a swallowing disorder. A gastrostomy–jejunostomy (G-J) tube was placed due to the risk of aspiration upon swallowing. Ibrutinib was started at a daily dose (QD) of 420 mg and administered through G-J tube.^{21,22} To promote biological availability, ibrutinib capsules were opened and dissolved in warm water, followed by administration via the G-J tube directly into the jejunum combined with continuous oral tube feeding (14 h/day). TDM was performed to ensure appropriate drug absorption and subsequent drug exposure. At 420 mg QD, the observed trough concentration (C_{trough}) was below the

quantification limit (Figure 1). An extended pharmacokinetic (PK) curve demonstrated a time to maximum concentration (T_{max}) of 1 h, followed by a constant level of 8 ug/L at 2–6 h. An overall exposure (AUC_{0-6h} of 48 ng*h/L) was estimated, suggesting low solubility and slow but sustained absorption compared to the PK profile in patients with chronic lymphoid leukaemia and healthy volunteers.^{23,24} Low ibrutinib concentrations were associated with a poor clinical response in this patient, as demonstrated by the persistence of high IgM levels. The dose of ibrutinib was increased to 280 mg twice a day to ensure continuous release. The ibrutinib plasma concentration remained below the target exposure; therefore, the dose was further increased to 280 mg 3 times a day (TID) and later to 420 mg TID, after which a response was achieved, as indicated by decreasing IgM levels. Upon TID dosing, we consulted the responsible gastroenterologist. Upon his advice, we trained the patient to dissolve ibrutinib in a small amount of tube feed and administered the drug–food combination via the gastric lumen to increase its solubility and improve gastric enzyme secretion. Follow-up serum levels were not conducted, as the patient unexpectedly passed away due to an event unrelated to Waldenström macroglobulinaemia.

Case 2: Dasatinib

A 35-year-old female with a history of a Roux-en-Y gastric bypass was diagnosed with BCR::ABL1-positive B-ALL. The patient was treated according to the standard arm of the paediatric-inspired HOVON 100 ALL protocol,²⁵ complicated by grade III hepatotoxicity. After recovery, treatment was switched to asparaginase and dasatinib. TDM was initiated to prevent toxicity and evaluate its efficacy. The primary targets of dasatinib TDM are C_{trough} and 2 h postdose (C_2) levels. Upon dose increase, C_{trough} only exceeded the target range once, but the C_2 concentration never reached the target concentration of >50 ng/mL (Figure 1).^{26–28} The increased C_2 concentrations on days 43 and 59 were due to interaction with isavuconazole, which was initiated because of invasive pulmonary aspergillosis. By day 66, we concluded that dasatinib malabsorption was the cause of low exposure. Considering the pH-dependent properties of dasatinib, with better dissolution in an acidic environment, pantoprazole was discontinued and dasatinib was administered at an increased dose of 200 mg QD with cola, as previously described for erlotinib.²⁹ Unfortunately, the results did not meet expectations. TDM showed a slight postadministration increase (C_2 concentration of 9 ng/mL), whereas C_{trough} remained relatively low, indicating that dissolution was the rate-limiting step for absorption. Subsequently, the dasatinib tablets were dissolved in cola before administration and the PK absorption curve was repeated. While the C_2 concentration remained below the target level, the overall exposure (AUC) increased 3-fold (Figure 1). Dasatinib

was temporarily discontinued due to severe pancytopenia. The patient achieved complete remission with no detectable measurable residual disease and undetectable BCR::ABL1, which was consolidated by allogeneic haematopoietic stem cell transplantation (HSCT). Dasatinib was restarted 4 months after allogeneic HSCT and patient continues to dissolve dasatinib in cola before ingestion. The patient is alive and well beyond 1 year after allogeneic HSCT.

3 | RESULTS

Two AI models were developed to predict the difference in molecular aqueous solubility between acid and neutral pH, to capture the concentration available for intestinal absorption in healthy and in patients with malabsorption issues.

3.1 | Modelling of chemical data to predict consequence of gastric bypass on TKIs

The neutral pH data were split based on scaffolds into training, validation and test subsets comprising 37 951, 5486 and 10 830 compounds, respectively, and randomly split into subsets comprising 37 870, 5437 and 10 960 compounds, respectively. The data corresponding to the difference in solubility between neutral and acidic pH ($\Delta\log S$) were similarly split into scaffold-based subsets of 96 456, 13 779 and 27 558 compounds, and random subsets of 96 520, 13 835 and 27 438 compounds, respectively.

The performances of the model predicting solubility at neutral pH (FCNN_{neutral}) and of the model predicting $\Delta\log S$ (FCNN _{$\Delta\log S$}) are reported in Table 1 (model, along with its instructions, is openly accessible on GitHub³⁰). As expected, using a scaffold split had an impact on the performance, as it was a tougher assessment of the models' extrapolation capabilities to new chemical series. Although this impact on the coefficient of correlation was large for

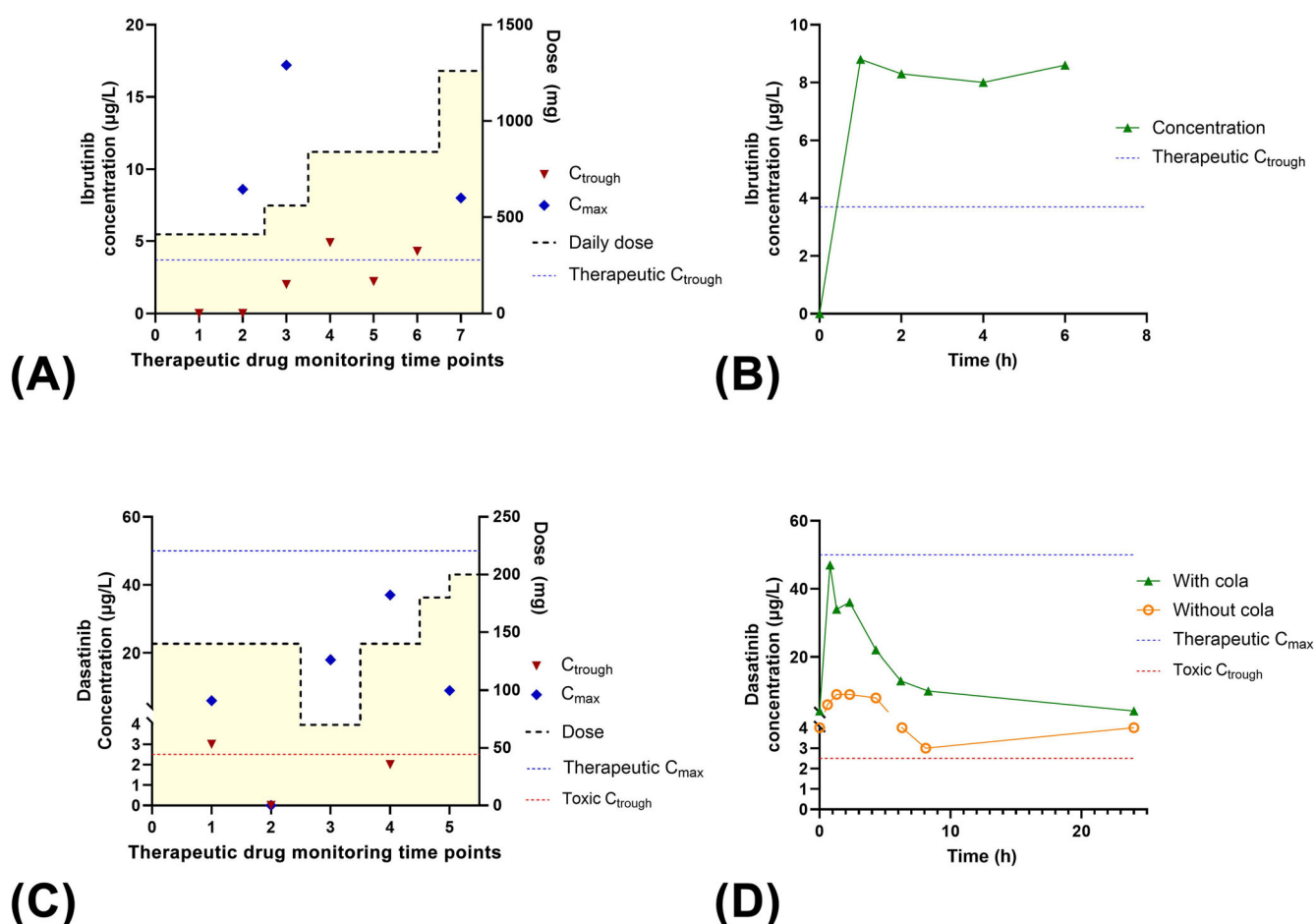


FIGURE 1 Drug dosing and concentration measurements in 2 patients with decreased GI absorption. The figures present the dosing and observed concentration–time curves during the concomitant administration of ibrutinib (a,b) and dasatinib (c,d) after stepwise adjustments that were made to optimize drug absorption and exposure. For a detailed description of the interventions, see Case 1: Ibrutinib and Case 2: Dasatinib in the case presentation section. The right panels present the steady-state concentration–time curves before (green) and after the intervention (orange). C_{max}, maximum concentration; C_{trough}, trough concentration.

TABLE 1 Model performance obtained at convergence. The number of epochs (each representing 1 complete pass through the training data) until the model stopped improving on the validation set are reported together with the mean square error (MSE), coefficient of determination (R^2) and Pearson's coefficient of correlation (Pearson's R) for both the training and test sets under both the data-leakage avoiding random and scaffold splitting schemes.

	Splitting scheme	No. of epochs	Training set			Validation set			Test set		
			MSE	R^2	Pearson's R	MSE	R^2	Pearson's R	MSE	R^2	Pearson's R
FCNN _{neutral}	random	1264	0.082	.790	.893	0.234	.421	.673	0.235	.417	.674
	scaffold	637	0.178	.548	.744	0.246	.369	.620	0.271	.304	.601
FCNN _{ΔlogS}	random	20 206	0.020	.988	.994	0.262	.898	.948	0.252	.900	.949
	scaffold	19 148	0.020	.989	.994	0.390	.842	.918	0.402	.832	.913

Abbreviation: FCNN = fully connected neural networks.

FCNN_{neutral} on the training set, it was much smaller for the validation and holdout test sets, with absolute differences of 0.149, 0.053 and 0.073, respectively. The FCNN_{neutral} model's performance on the test set was still limited, with a coefficient of determination R^2 of .417 on the test set, but its Pearson coefficient of correlation of .674 was used to give an indication of a compound's solubility at neutral pH.

Surprisingly, the performance of the FCNN_{ΔlogS} model was almost independent of the splitting scheme used, with differences in Pearson correlation coefficients of .000, .056 and .036 for the training, validation and holdout test sets, respectively. Furthermore, the coefficient of correlation obtained under a scaffold split was very high (.913), highlighting the model's ability to extrapolate to new molecular series, whereas those obtained under the random splitting scheme demonstrated strong interpolation capabilities with a correlation coefficient of .949.

Randomly split models were chosen for predictions because they learned a more balanced distribution of molecular features than their scaffold split counterparts. Solubilities at pH 1.0 ($-\log S$ pH = 1.0) were estimated from the summed predictions of both the models.

The AI-predicted changes in solubility between neutral and acidic pH correlate with clinical effects on bioavailability, as reflected by changes in AUC due to PPI use for each TKI are presented in Figure 2. Compounds near the regression line are well predicted, while the model's false positives and false negatives are identified in specific quadrants based on their PPI impact on absorption. The top 10 TKIs with the greatest AI-predicted decrease in solubility at elevated pH and their corresponding clinical impact on bioavailability are summarized in Table 2.

3.2 | Clinical validation of model results

None of the BCS classification groups (I/II/III/IV) significantly differed in terms of their median predicted solubility (Kruskal–Wallis H -test and ANOVA) at either pH or their median difference in solubility (Table S1). Interestingly, only 21 of the 71 TKIs fell under Lipinski's rule of 5, predictive for adequate absorption.

The predicted solubility at neutral pH did not significantly differ across groups of pH-dependent solubility (Mann–Whitney U -test) but did differ both for solubility at acidic pH ($P < .003$) and the predicted difference in solubility ($P < .003$, Table S1).

The medians of the predicted solubility at neutral pH, predicted solubility at acidic pH and difference in solubility were all significantly different among the groups of low and medium acid-suppressive agents (Mann–Whitney U -test and Student t -test $P = .001$; .003; <.001, respectively). Furthermore, logistic regression further characterized the relationship between the predicted $\Delta\log S$ and the pH-dependent solubility groups and groups of low and medium acid-suppressive agents with odds ratios of 3.97 and 6.10, respectively (Table S2).

The predicted change in solubility due to the pH shift was positive for 7 of the 8 acids in the model, suggesting a slight increase in exposure due to concomitant PPI administration (Figure S1; Appendix). Indeed, in the clinical data (Summary of Product Characteristics), these drugs showed only a limited antiacid effect on bioavailability (Appendix). This clinical validation demonstrates the model's direct applicability in patient care, enabling adjustments to drug administration, such as the alternative dissolving strategies described in Case 1 (Box).

4 | DISCUSSION

4.1 | AI-based prediction of TKI bioavailability

In this study, we developed an AI-based model to predict the risk of reduced bioavailability for TKIs in patients with altered gastric conditions. The model correlated well with the predicted difference in solubility between acidic and neutral pH and the clinical bioavailability when exposed to gastric acid suppressants. This is particularly relevant for patients who have undergone bariatric surgery or those receiving PPIs, as their altered gastric environments can significantly impact drug solubility and absorption. Traditional models, such as Lipinski's rule of 5, no longer apply to most newly licensed TKIs, suggesting that new models are needed to predict the absorption of compounds in such patients. Additionally, we share our experience

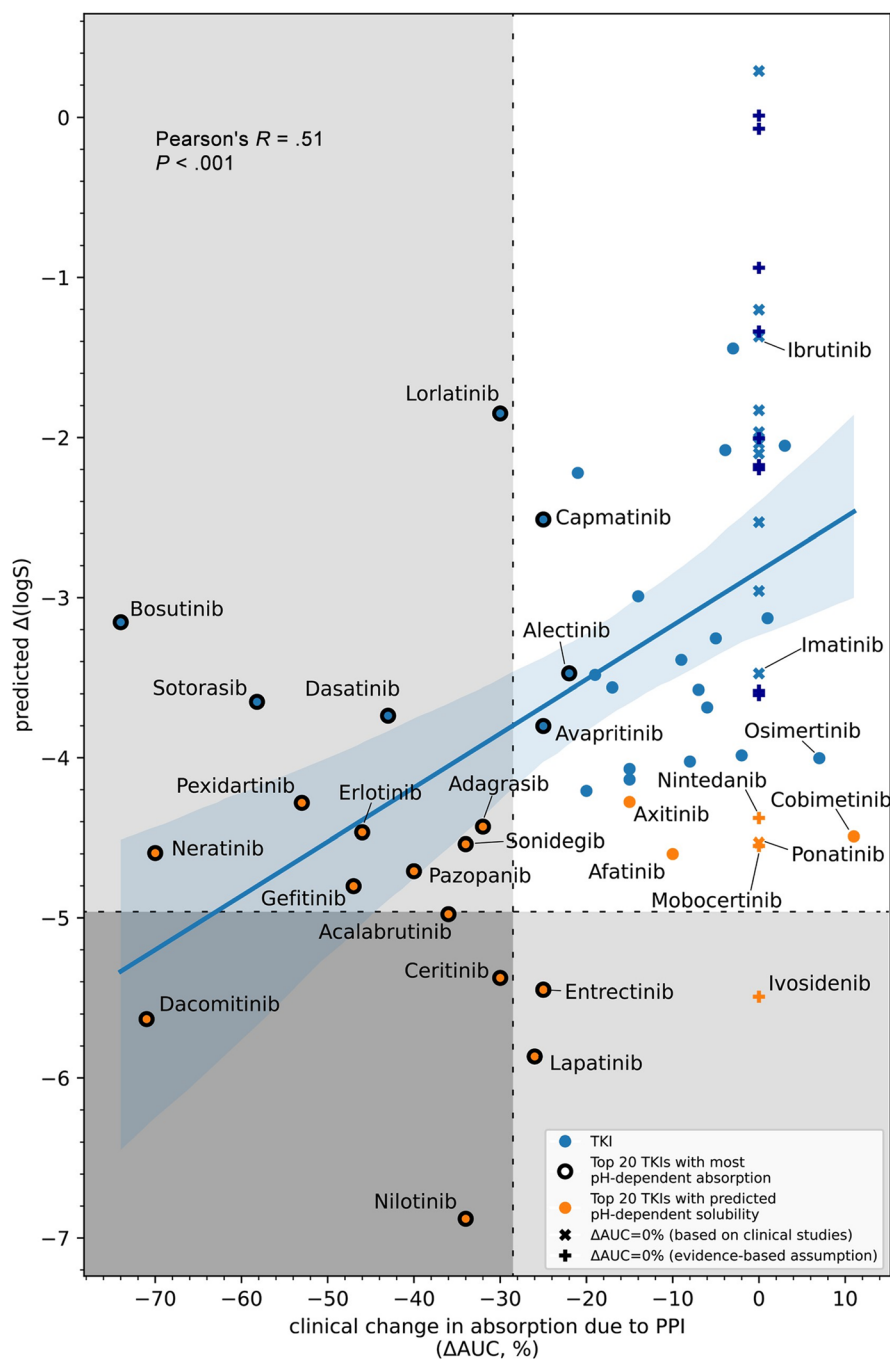


FIGURE 2 Correlation between artificial intelligence-predicted solubility shifts and clinical pH-dependent bioavailability changes. The x-axis shows log-normalized changes in solubility (acidic vs. neutral pH) predicted by the FCNN $_{\Delta \log S}$ model. The y-axis shows the percent change in AUC observed with proton-pump inhibitor (PPI) coadministration, based on regulatory assessments (FDA, EMA, TGA) and clinical trials (see Appendix). Each point represents a tyrosine kinase inhibitor (TKI). Compounds lying close to the regression line (blue line) and within the confidence interval are predicted well by the model throughout the pH-dependent solubility range. The horizontal shaded area contains TKIs, for which the FCNN $_{\Delta \log S}$ model predicts lower solubility at increased pH. The vertical shaded area contains compounds for which absorption is most affected by PPI. The darker lower left-hand corner highlights TKIs (orange points with black outline) whose PPI influence on absorption is associated with the FCNN $_{\Delta \log S}$ model predictions. The upper-left quadrant contains compounds for which the clinically relevant impact of PPI on absorption was missed by the FCNN $_{\Delta \log S}$ model (false negatives; blue points with black outline). The lower-right quadrant contains TKIs the FCNN $_{\Delta \log S}$ model prioritizes with no clinically significant PPI effect on absorption (false positives; orange points). The top-right quadrant contains TKIs for which the FCNN $_{\Delta \log S}$ model's predictions are well associated with the limited impact of PPI on absorption. Compounds with change in the area under the concentration–time curve (ΔAUC) = 0% fall into 2 categories: those for which clinical studies reported overlapping confidence intervals for AUC with and without PPI, and those with no expected PPI interaction based on regulatory documents or preclinical data. These are included in the analysis and did not differ significantly in physicochemical properties compared to the rest of the dataset. TKI with $\Delta AUC = 0\%$ fall into 2 categories: those for which clinical studies reported overlapping confidence intervals for AUC with and without PPI (crosses), and those with no expected PPI interaction based on regulatory documents or preclinical data (dark blue plus signs).

TABLE 2 Top 10 tyrosine kinase inhibitors (TKIs) with the greatest artificial intelligence-predicted decrease in solubility at elevated pH and their corresponding clinical impact on bioavailability.

	TKI	Predicted $\Delta\log S$	pH-dependent ΔAUC
1.	Nilotinib	-6,88	-34%
2.	Lapatinib	-5,87	-26%
3.	Dacomitinib	-5,63	-71%
4.	Ivosidenib	-5,49	0%
5.	Entrectinib	-5,45	-25%
6.	Ceritinib	-5,38	-30%
7.	Acalabrutinib	-4,98	-36%
8.	Infigratinib	-4,86	unknown
9.	Gefitinib	-4,8	-47%
10.	Pazopanib	-4,71	-40%

Abbreviation: AUC = area under the concentration–time curve.

with 2 patients who presented with GI problems of TKI absorption and dissolution in cola or oral tube feeding as a method to overcome the reduced bioavailability due to high gastric pH.

4.2 | TDM and its role in optimizing TKI exposure

Optimizing drug exposure using TDM is a major determinant of the therapeutic success of TKIs, which require long-term oral treatment in the context of chronic GI disturbances that affect TKI bioavailability. Using TDM, drug concentrations are measured in serum samples obtained from patients in order to optimize drug dosing. Implementation of TDM to assess reduced bioavailability is feasible because target therapeutic concentrations of most TKIs are available in literature.¹³ As an alternative, the reference median concentration–time profile at the optimum dose can be assessed through drug filing information (e.g., for newer TKIs, in which exposure–response relationships have not yet been fully established for real-world patients). TDM for TKIs is typically performed at specialized centres using various analytical techniques, with liquid chromatography–mass spectrometry as the reference method,^{31,32} allowing rapid evaluation of bioavailability in an individual patient and timely dose adjustments if needed. Concentrations of multiple TKIs have been linked to efficacy and toxicity, specifically in cases of expected alterations in absorption, distribution, metabolism and excretion, DDIs and disease.¹³ However, with some exceptions, such as imatinib for chronic myeloid leukaemia and GI stromal tumour patients, TDM remains infrequently applied. Therefore, implementation of our proposed methodology would enhance treatment efficacy and increase the need for dedicated TKI PK-sampling facilities.

4.3 | Strategies to overcome TKI malabsorption

For TKIs, which are dependent on a low intragastric pH for their solubility and, hence, absorption, several strategies can be used to boost their absorption.

4.3.1 | Adjusting gastric pH management

If elevated intragastric pH is caused by a PPI, switching to a short-acting antacid or TKI that is less dependent on low intragastric pH is recommended. If TKI switching is not an option, a once-daily dosing regimen and application of a time interval between drug administrations may be an option.⁵ Administration of the gastric-acid suppressant 1–2 h after the intake of the TKI may enable the TKI to dissolve at the lowest pH.^{5,33}

4.3.2 | Alternative drug administration techniques

However, despite optimizing the dosing interval, absorption may still be significantly decreased.³³ Therefore, it is essential to evaluate drug exposure and develop additional strategies. In case of a physiological cause of malabsorption, such as achlorhydria, a bypass or complete removal of the stomach, the solubility can be increased by crushing the tablet or capsule or dissolving the tablet or capsule prior to administration.^{34,35} The gastroenterologist may advise to administer the drug into the gastric lumen using a nasoduodenal feeding tube.

4.3.3 | Use of acidic solvents

Solubility and absorption can be further improved by using a (buffered) acidic solution to mimic low intragastric pH conditions.^{29,36,37} Most studies have been performed with classic Coca-Cola as this formulation has the lowest pH, is well preserved and widely available, which aids reproducibility.^{29,38–40} However, the contribution of sugar components and buffering capacity remains unclear. The role of sugar in the GI system is complex, as high blood glucose may decrease gastric acid secretion, whereas energy-dense carbonated soft drinks may decrease gastric pH and delay gastric emptying.^{41,42} With regard to buffering capacity, diet formulations of popular cola drinks may be preferred over classic Coca-Cola.⁴³ If acidity is the main determining factor, healthier alternatives, such as orange juice or (sugar-free) lemonade may be preferred. For some TKIs, administration with a meal can enhance solubility because of the fats present in food.⁴⁴ In addition, food intake can stimulate postprandial gastric acid secretion and bile salts, which can also aid solubility and hence absorption.^{45,46}

4.3.4 | Pharmacokinetic approaches

For TKIs with solubility-limited absorption, such as nilotinib, dividing the daily dose over multiple doses (split-dose administration) will result in higher levels of absorption than increasing the dose alone.⁴⁷ Another approach to enhance drug exposure is by making use of pharmacokinetic DDIs, also known as pharmacokinetic boosting. This can be investigated for TKIs with a preferred route of metabolism via

CYP3A4. By intentionally combining a CYP3A4 inhibitor, such as cobicistat or ritonavir, with a TKI, drug metabolism decreases and drug exposure to the TKI parent compound increases. Tdm can be a necessary value in guiding boosted regimens and monitoring their efficacy and toxicity.^{48–50} However, CYP3A4 inhibitors are well known for their DDIs with other compounds beyond boosting the intended TKI treatment. Therefore, this strategy presents new risks to patients. In the case of the second patient presented here, treatment with a CYP3A4 inhibitor to boost TKI exposure would have risked causing unintentional toxicity, as this patient concomitantly used vincristine, etoposide and oxycodone; 3 CYP3A4 substrates with a small therapeutic window.

4.3.5 | Formulation based solutions

In addition, modifying the formulation of a TKI with low solubility may increase its bioavailability. Several strategies can increase the water solubility of poorly soluble TKIs, such as the use of prodrugs, polymeric nanoparticles, lipoidal microspheres, solubilizers and amorphous solid dispersions,⁵¹ none of which are captured by the AI model. The latter approach is deemed the most successful, and has been used for the formulation of vemurafenib and regorafenib.⁵² However, pH seemed to have little impact on either drug. In addition, complexation with cyclodextrins as is used for the IV formulation of voriconazole could theoretically also improve the solubility of lipophilic TKIs, thereby reducing the effect of pKa on solubility.⁵³ This could be an option to explore when administration via a narrow nasogastric tube or percutaneous endoscopic gastrostomy tube is needed, or when testing other routes of administration (SC, IV).

4.4 | Limitations of the AI model and future directions

A disadvantage of our modelling effort is that enhancing solubility by reformulation reduces the predictability of our model. Reformulation may have resulted in the poor predictive value of some TKIs in our model. Other causes of some poor predictions by the model, such as nilotinib and lapatinib, this may be caused by saturable absorption or due to interaction with efflux transporters but should be studied further. Other model's limitations include the limited extrapolation to novel TKIs with unconventional pharmacokinetics, such as nilotinib and sorafenib that exhibit nonproportional increases in exposure with dose escalation, due to factors such as transporter (P-glycoprotein)-mediated interactions, first pass metabolism and time dependent inhibition of P450 cytochrome enzyme activity.⁵⁴ Future prospective validation of the model by prospective monitoring of the effect of dissolving TKIs in cola on clinical exposure would reinforce the AI model's reliability and its practical application in the clinical setting.^{48–50}

4.5 | Clinical implications and need for guidelines

The incidence of erratic drug absorption among patients has recently risen, attributed to the growing population with prior GI surgeries such as gastric bypass or gastrectomy, often performed for conditions such as obesity or gastric cancer.^{55,56} This increase is associated with advancing age and lifestyle factors such as diet, obesity and lack of physical activity. Furthermore, the number of patients using TKIs has increased, due to advancements in targeted therapies, many new drug approvals, expanded indications and the rise in molecular and genetic testing. Therefore, there is an urgent need to develop guidelines for predicting, monitoring and boosting bioavailability, and the current manuscript provides the first step towards such a guideline.

5 | CONCLUSIONS

In clinical practice, the bioavailability of TKIs can be challenging in patients with GI malabsorption due to feeding tubes or gastric bypass surgery. In a multidisciplinary approach, we defined different strategies to enhance the bioavailability of TKIs. An AI-based model was created to predict TKIs that are at risk of malabsorption when bypassing the stomach or coadministered with PPIs. This model can be used to predict the differences in solubility between acidic and neutral pH and the bioavailability of TKIs when exposed to PPIs.

AUTHOR CONTRIBUTIONS

Daan W. Huntjens: Conceptualization; data curation; formal analysis; investigation; writing—original draft preparation. **Olivier J. M. Béquignon:** Data curation; formal analysis; investigation; methodology; software; validation; visualization; writing—original draft preparation. **Stefanie D. Krens:** Conceptualization; data curation; writing—original draft preparation. **Mark Löwenberg:** Supervision; writing—review and editing. **Martine E.D. Chamuleau:** Investigation; supervision; writing—review and editing. **Remco J. Molenaar:** Investigation; writing—review and editing. **Anita M.G. Kramers:** Investigation; writing—review and editing. **Marianne A. Kuijvenhoven:** Conceptualization; data curation; formal analysis; investigation; supervision; writing—original draft preparation. **Imke H. Bartelink:** Conceptualization; data curation; investigation; methodology; supervision; writing—original draft preparation.

ACKNOWLEDGEMENTS

We would like to acknowledge the contributions of hospital pharmacists in training, M. Slijkhuis and M.D. Rombouts, as well as gastroenterologist in training, L.K. Wanders.

CONFLICT OF INTEREST STATEMENT

The authors state that this research was conducted without any commercial or financial ties that could be interpreted as potential conflicts of interest. However, outside of this research, the following authors declare the following:

M.L.O.W.: consultancy/lecture fees from Abbvie, Bristol Myers Squibb, Eli Lilly, Galapagos, Janssen-Cilag, Johnson & Johnson, Medtronic, Pfizer, Takeda, Tillotts. Central reader for Alimentiv. Grants received from Galapagos, Pfizer, ZonMW and NFU transformation deal.

S.D.K. received speaker honoraria from GSK.

M.C.H.: research support AbbVie, GenMab, BMS. Consultancy AbbVie, BYON, Novartis.

I.H.B.: grants received from KWF, Gardenia (Amsterdam UMC).

DATA AVAILABILITY STATEMENT

The raw data that support the findings of this study are available from the corresponding author, D.W.H., upon reasonable request. The model that supports the findings of this study is openly available on GitHub at <https://github.com/OlivierBeq/SolpHedge>. This includes instructions on how to run the model and obtain results.

PATIENT CONSENT STATEMENT

Written informed consent has been obtained from the involved patients, and they have given approval for this information to be published in this article.

ORCID

Daan W. Huntjens  <https://orcid.org/0000-0001-5354-9935>

Olivier J. M. Béquignon  <https://orcid.org/0000-0002-7554-9220>

Stefanie D. Krens  <https://orcid.org/0000-0002-4406-7149>

Mark Löwenberg  <https://orcid.org/0000-0002-4975-9945>

Martine E. D. Chamuleau  <https://orcid.org/0000-0002-0123-9182>

Remco J. Molenaar  <https://orcid.org/0000-0001-5651-3997>

Marianne A. Kuijvenhoven  <https://orcid.org/0000-0001-7125-2449>

Imke H. Bartelink  <https://orcid.org/0000-0001-9602-3407>

REFERENCES

- Cohen P, Cross D, Janne PA. Kinase drug discovery 20 years after imatinib: progress and future directions. *Nat Rev Drug Discov*. 2021; 20(7):551-569. doi:10.1038/s41573-021-00195-4
- Ferrer F, Tetu P, Dousset L, et al. Tyrosine kinase inhibitors in cancers: treatment optimization - part II. *Crit Rev Oncol Hematol*. 2024;200: 104385. doi:10.1016/j.critrevonc.2024.104385
- Martinez MN, Amidon GL. A mechanistic approach to understanding the factors affecting drug absorption: a review of fundamentals. *J Clin Pharmacol*. 2002;42(6):620-643. doi:10.1177/00970002042006005
- Smidova V, Michalek P, Goliasova Z, et al. Nanomedicine of tyrosine kinase inhibitors. *Theranostics*. 2021;11(4):1546-1567. doi:10.7150/thno.48662
- van Leeuwen RWF, Jansman FGA, Hunfeld NG, et al. Tyrosine kinase inhibitors and proton pump inhibitors: an evaluation of treatment options. *Clin Pharmacokinet*. 2017;56(7):683-688. doi:10.1007/s40262-016-0503-3
- Benet LZ. The role of BCS (biopharmaceutics classification system) and BDDCS (biopharmaceutics drug disposition classification system) in drug development. *J Pharm Sci*. 2013;102(1):34-42. doi:10.1002/jps.23359
- Sorkun MC, Khetan A, Er S. AqSolDB, a curated reference set of aqueous solubility and 2D descriptors for a diverse set of compounds. *Sci Data*. 2019;6(1):143. doi:10.1038/s41597-019-0151-1
- Cui Q, Lu S, Ni B, et al. Improved prediction of aqueous solubility of novel compounds by going deeper with deep learning. *Front Oncol*. 2020;10:121. doi:10.3389/fonc.2020.00121
- Deng C, Liang L, Xing G, et al. Multi-channel GCN ensemble machine learning model for molecular aqueous solubility prediction on a clean dataset. *Mol Divers*. 2023;27(3):1023-1035. doi:10.1007/s11030-022-10465-x
- Panapitiya G, Girard M, Hollas A, et al. Evaluation of deep learning architectures for aqueous solubility prediction. *ACS Omega*. 2022; 7(18):15695-15710. doi:10.1021/acsomega.2c00642
- Zhu T, Chen Y, Tao C. Multiple machine learning algorithms assisted QSPR models for aqueous solubility: comprehensive assessment with CRITIC-TOPSIS. *Sci Total Environ*. 2023;857(Pt 2):159448. doi:10.1016/j.scitotenv.2022.159448
- Bonin A, Montanari F, Niederfuhr S, Goller AH. pH-dependent solubility prediction for optimized drug absorption and compound uptake by plants. *J Comput Aided Mol des*. 2023;37(3):129-145. doi:10.1007/s10822-023-00496-3
- Mueller-Schoell A, Groenland SL, Scherf-Clavel O, et al. Therapeutic drug monitoring of oral targeted antineoplastic drugs. *Eur J Clin Pharmacol*. 2021;77(4):441-464. doi:10.1007/s00228-020-03014-8
- Sushko I, Novotarskyi S, Korner R, et al. Online chemical modeling environment (OCHEM): web platform for data storage, model development and publishing of chemical information. *J Comput Aided Mol Des*. 2011;25(6):533-554. doi:10.1007/s10822-011-9440-2
- Hong H, Xie Q, Ge W, et al. Mold(2), molecular descriptors from 2D structures for chemoinformatics and toxicoinformatics. *J Chem Inf Model*. 2008;48(7):1337-1344. doi:10.1021/ci800038f
- Yap CW. PaDEL-descriptor: an open source software to calculate molecular descriptors and fingerprints. *J Comput Chem*. 2011;32(7): 1466-1474. doi:10.1002/jcc.21707
- Cao DS, Xu QS, Hu QN, Liang YZ. ChemoPy: freely available python package for computational biology and chemoinformatics. *Bioinformatics*. 2013;29(8):1092-1094. doi:10.1093/bioinformatics/btt105
- Willighagen EL, Mayfield JW, Alvarsson J, et al. The chemistry development kit (CDK) v2.0: atom typing, depiction, molecular formulas, and substructure searching. *J Chem*. 2017;9(1):33. doi:10.1186/s13321-017-0220-4
- Bequignon OJM. Papyrus structure pipeline. https://github.com/OlivierBeq/Papyrus_structure_pipeline
- Rodgers T, Rowland M. Physiologically based pharmacokinetic modelling 2: predicting the tissue distribution of acids, very weak bases, neutrals and zwitterions. *J Pharm Sci*. 2006;95(6):1238-1257. doi:10.1002/jps.20502
- Maddox JM, Majid M. Use of ibuprofen via nasogastric (NG) Tube & Percutaneous Endoscopic Gastrostomy (PEG) tube. *Blood*. 2016; 128(22):5371. doi:10.1182/blood.V128.22.5371.5371
- Alsuliman T, Belghoul M, Choufi B. Ibuprofen treatment through nasogastric tube in a comatose patient with central nervous system localization of mantle cell lymphoma. *Case Rep Hematol*. 2018;2018: 5761627. doi:10.1155/2018/5761627
- Research FCFDEa. Clinical pharmacology and biopharmaceutics review(s) ibuprofen; 2013. https://www.accessdata.fda.gov/drugsatfda_docs/nda/2013/205552Orig1s000ClinPharmR.pdf
- Calleja A, De Barros S, Vinson C, et al. Interest of dosing of ibuprofen in B-cell lymphoid malignancies: data from a real-life, phase 4 study. *Blood*. 2018;132(Supplement 1):3960. doi:10.1182/blood-2018-99-116532
- Rijneveld AW, van der Holt B, de Weerd O, et al. Clofarabine added to intensive treatment in adult patients with newly diagnosed ALL: the HOVON-100 trial. *Blood Adv*. 2022;6(4):1115-1125. doi:10.1182/bloodadvances.2021005624
- Wang X, Hochhaus A, Kantarjian HM, et al. Dasatinib pharmacokinetics and exposure-response (E-R): relationship to safety and efficacy in

- patients (pts) with chronic myeloid leukemia (CML). *J Clin Oncol*. 2008;26(15_suppl):3590-3590. doi:10.1200/jco.2008.26.15_suppl.3590
27. Shah NP, Nicoll JM, Bleickardt E, Nicaise C, Paquette RL, Sawyers CL. Potent transient inhibition of BCR-ABL by Dasatinib leads to complete cytogenetic remissions in patients with chronic myeloid leukemia: implications for patient management and drug development. *Blood*. 2006;108(11):2166-2166. doi:10.1182/blood.V108.11.2166.2166
 28. Yu H, Steeghs N, Nijenhuis CM, Schellens JH, Beijnen JH, Huitema AD. Practical guidelines for therapeutic drug monitoring of anticancer tyrosine kinase inhibitors: focus on the pharmacokinetic targets. *Clin Pharmacokinet*. 2014;53(4):305-325. doi:10.1007/s40262-014-0137-2
 29. van Leeuwen RW, Peric R, Hussaarts KG, et al. Influence of the acidic beverage cola on the absorption of erlotinib in patients with non-small-cell lung cancer. *J Clin Oncol*. 2016;34(12):1309-1314. doi:10.1200/JCO.2015.65.2560
 30. OJM B. pH-dependent solubility predictions for small molecules. <https://github.com/OlivierBeq/SolpHedge>
 31. Herviou P, Thivat E, Richard D, et al. Therapeutic drug monitoring and tyrosine kinase inhibitors. *Oncol Lett*. 2016;12(2):1223-1232. doi:10.3892/ol.2016.4780
 32. Verougstraete N, Stove V, Verstraete AG, Stove CP. Therapeutic drug monitoring of tyrosine kinase inhibitors using dried blood microsamples. *Front Oncol*. 2022;12:821807. doi:10.3389/fonc.2022.821807
 33. Krens SD, Lubberman FJE, van Egmond M, et al. The impact of a 1-hour time interval between pazopanib and subsequent intake of gastric acid suppressants on pazopanib exposure. *Int J Cancer*. 2021;148(11):2799-2806. doi:10.1002/ijc.33469
 34. Heath EI, Forman K, Malburg L, et al. A phase I pharmacokinetic and safety evaluation of oral pazopanib dosing administered as crushed tablet or oral suspension in patients with advanced solid tumors. *Invest New Drugs*. 2012;30(4):1566-1574. doi:10.1007/s10637-011-9725-2
 35. Bernsen EC, Hogenes VJ, Nuijen B, Hanff LM, Huitema ADR, Diekstra MHM. Practical recommendations for the manipulation of kinase inhibitor formulations to age-appropriate dosage forms. *Pharmaceutics*. 2022;14(12):2834. doi:10.3390/pharmaceutics14122834
 36. Knoebel RW, Larson RA. Pepsi® or coke®? Influence of acid on dasatinib absorption. *J Oncol Pharm Pract*. 2018;24(2):156-158. doi:10.1177/1078155217692152
 37. Muhammad HJ, Shimada T, Fujita A, Sai Y. Sodium citrate buffer improves pazopanib solubility and absorption in gastric acid-suppressed rat model. *Drug Metab Pharmacokinet*. 2024;55:100995. doi:10.1016/j.dmpk.2024.100995
 38. Reddy A, Norris DF, Momeni SS, Waldo B, Ruby JD. The pH of beverages in the United States. *J Am Dent Assoc*. 2016;147(4):255-263. doi:10.1016/j.adaj.2015.10.019
 39. Jaruratanasirikul S, Kleepkaew A. Influence of an acidic beverage (Coca-Cola) on the absorption of itraconazole. *Eur J Clin Pharmacol*. 1997;52(3):235-237. doi:10.1007/s002280050280
 40. Chin TW, Loeb M, Fong IW. Effects of an acidic beverage (Coca-Cola) on absorption of ketoconazole. *Antimicrob Agents Chemother*. 1995;39(8):1671-1675. doi:10.1128/AAC.39.8.1671
 41. Moore JG. Gastric acid suppression by intravenous glucose solutions. *Gastroenterology*. 1973;64(6):1106-1110. doi:10.1016/S0016-5085(73)80064-2
 42. Leiper JB. Fate of ingested fluids: factors affecting gastric emptying and intestinal absorption of beverages in humans. *Nutr Rev*. 2015;73(Suppl 2):57-72. doi:10.1093/nutrit/nuv032
 43. Borjian A, Ferrari CC, Anouf A, Touyz LZ. Pop-cola acids and tooth erosion: an in vitro, in vivo, electron-microscopic, and clinical report. *Int J Dent*. 2010;2010:957842. doi:10.1155/2010/957842
 44. Veerman GDM, Hussaarts K, Jansman FGA, Koolen SWL, van Leeuwen RWF, Mathijssen RHJ. Clinical implications of food-drug interactions with small-molecule kinase inhibitors. *Lancet Oncol*. 2020;21(5):e265-e279. doi:10.1016/S1470-2045(20)30069-3
 45. Pavlovic N, Golocorbin-Kon S, Ethnic M, et al. Bile acids and their derivatives as potential modifiers of drug release and pharmacokinetic profiles. *Front Pharmacol*. 2018;9:1283. doi:10.3389/fphar.2018.01283
 46. Stillhart C, Vucicevic K, Augustijns P, et al. Impact of gastrointestinal physiology on drug absorption in special populations--an UNGAP review. *Eur J Pharm Sci*. 2020;147:105280. doi:10.1016/j.ejps.2020.105280
 47. Tanaka C, Yin OQ, Sethuraman V, et al. Clinical pharmacokinetics of the BCR-ABL tyrosine kinase inhibitor nilotinib. *Clin Pharmacol Ther*. 2010;87(2):197-203. doi:10.1038/clpt.2009.208
 48. Hofman S, Touw DJ, Span BFR, Munnink TO. Cobicicistat as a potential booster of ponatinib and Dasatinib exposure in a CML patient: a case study. *Ther Drug Monit*. 2023;45(4):428-430. doi:10.1097/Ftd.0000000000001103
 49. Westra N, Touw D, Hooge M, Kosterink J, Munnink TO. Pharmacokinetic boosting of kinase inhibitors. *Pharmaceutics*. 2023;15(4):1149. doi:10.3390/pharmaceutics15041149
 50. ClinicalTrials.gov. A trial to assess cobicicistat boosted venetoclax in combination with azacitidine in adult patients with newly diagnosed AML (HO171). National Library of Medicine. <https://clinicaltrials.gov/study/NCT06014489>
 51. Gala UH, Miller DA, Williams RO 3rd. Harnessing the therapeutic potential of anticancer drugs through amorphous solid dispersions. *Biochim Biophys Acta Rev Cancer*. 2020;1873(1):188319. doi:10.1016/j.bbcan.2019.188319
 52. Herbrink M, Schellens JH, Beijnen JH, Nuijen B. Inherent formulation issues of kinase inhibitors. *J Control Release*. 2016;239:118-127. doi:10.1016/j.jconrel.2016.08.036
 53. Conceicao J, Adeoye O, Cabral-Marques HM, Lobo JMS. Cyclodextrins as drug carriers in pharmaceutical technology: the state of the art. *Curr Pharm des*. 2018;24(13):1405-1433. doi:10.2174/1381612824666171218125431
 54. Rowland A, van Dyk M, Mangoni AA, et al. Kinase inhibitor pharmacokinetics: comprehensive summary and roadmap for addressing inter-individual variability in exposure. *Expert Opin Drug Metab Toxicol*. 2017;13(1):31-49. doi:10.1080/17425255.2016.1229303
 55. Surgery ASfMaB. Estimate of bariatric surgery numbers, 2011-2022. <https://asmb.org/resources/estimate-of-bariatric-surgery-numbers/>
 56. Lu L, Mullins CS, Schafmayer C, Zeissig S, Linnebacher M. A global assessment of recent trends in gastrointestinal cancer and lifestyle-associated risk factors. *Cancer Commun (Lond)*. 2021;41(11):1137-1151. doi:10.1002/cac2.12220

SUPPORTING INFORMATION

Additional supporting information can be found online in the Supporting Information section at the end of this article.

How to cite this article: Huntjens DW, Béquignon OJM, Krens SD, et al. Artificial intelligence modelling of tyrosine kinase inhibitors at risk of malabsorption and bioavailability-enhancing strategies. *Br J Clin Pharmacol*. 2025;91(11):3130-3140. doi:10.1002/bcp.70166